PROCEEDINGS OF SCIENCE

QED corrections to hadronic processes: a strategy for lattice QCD

N. Carrasco [a], **V. Lubicz*** [a], **G. Martinelli** [b], **C.T. Sachrajda** [c], **N. Tantalo** [d], **C. Tarantino** [a], **M. Testa** [b]

[a] *Dipartimento di Matematica e Fisica, Università Roma Tre and INFN, Sezione di Roma Tre, Via della Vasca Navale 84, I-00146 Rome, Italy*
[b] *Dipartimento di Fisica, Università di Roma La Sapienza and INFN Sezione di Roma, Piazzale Aldo Moro 5, 00185 Roma, Italy*
[c] *School of Physics and Astronomy, University of Southampton, Southampton SO17 1BJ, UK*
[d] *Dipartimento di Fisica, Università di Roma Tor Vergata and INFN, Sezione di Tor Vergata, I-00133 Rome, Italy*

E-mail: carrasco@fis.uniroma3.it, lubicz@fis.uniroma3.it, guido.martinelli@roma1.infn.it, cts@soton.ac.uk, nazario.tantalo@roma2.infn.it, tarantino@fis.uniroma3.it, massimo.testa@roma1.infn.it

Recently, a method has been proposed [1] for the first time to compute electromagnetic effects in hadronic processes using lattice simulations. The method can be applied, for example, to the leptonic and semileptonic decays of light or heavy pseudoscalar mesons. For these quantities the presence of infrared divergences in intermediate stages of the calculation makes the procedure more complicated than is the case for the hadronic spectrum, for which lattice calculations already exist. In this talk, I illustrate the method for the leptonic decays of a pseudoscalar meson. Its practical implementation, although challenging, is within reach of the present lattice technology and preliminary numerical results are presented at this conference.

*The 8th International Workshop on Chiral Dynamics, CD2015 ****
29 June 2015 - 03 July 2015
Pisa, Italy

*Speaker.

PoS(CD15)023

1. Introduction

Precision flavour physics is a particularly powerful tool for exploring the limits of the Standard Model (SM) of particle physics and in searching for inconsistencies which would signal the existence of new physics. An important component of this endeavour is the over-determination of the elements of the Cabibbo-Kobayashi-Maskawa (CKM) matrix from a wide range of weak processes. The precision in extracting CKM matrix elements is generally limited by our ability to quantify hadronic effects and the main goal of large-scale simulations using the lattice formulation of QCD is the *ab-initio* evaluation of the non-perturbative QCD effects in physical processes. The recent, very impressive, improvement in lattice computations has led to a precision approaching $O(1\%)$ for a number of quantities (see e.g. Ref. [2] and references therein) and therefore in order to make further progress electromagnetic effects (and other isospin-breaking contributions) have to be considered. The question of how to include electromagnetic effects in the hadron spectrum and in the determination of quark masses in ab-initio lattice calculations was addressed for the first time in [3]. Much theoretical and algorithmic progress has been made following this pioneering work, particularly in recent years, leading to remarkably accurate determinations of the charged-neutral mass splittings of light pseudoscalar mesons and light baryons (see Refs. [4, 5, 6, 7, 8, 9] for recent papers on the subject and Refs. [10, 11] for reviews of these results and a discussion of the different approaches used to perform QED+QCD lattice calculations of the spectrum).

In the spectrum calculations, two main approaches have been pursued. The direct one consists in adding the electromagnetic interaction to the quark action [3, 4, 5, 7, 8, 9]. A different method, developed in Ref. [6], is based on a combined expansion of the lattice path integral in powers of the light quark mass difference $(m_d - m_u)$ and the electromagnetic coupling α. This method relies on the observation that isospin breaking effects, including those associated with QED interactions, are tiny because very small factors, $(m_d - m_u)/\Lambda_{QCD}$ and α, multiply sizable matrix elements of hadronic operators. An advantage of this method with respect to the standard approach is that, by working at fixed order in a perturbative expansion, one is able to factorize the small coefficients and to get relatively large numerical signals. For the same reason, one does not need to perform simulations at unphysical values of the electric charge, thus avoiding extrapolations of the lattice data with respect to α.

In the computation of the hadron spectrum there is a very significant simplification in that there are no infrared divergences. In Ref. [1] we have proposed a strategy to include electromagnetic effects in processes for which infrared divergences are present but which cancel in the standard way between diagrams containing different numbers of real and virtual photons [12]. The presence of infrared divergences in intermediate steps of the calculation requires the development of new methods. Indeed, in order to cancel the infrared divergences and obtain results for physical quantities, radiative corrections from virtual and real photons must be combined. We stress that it is not sufficient simply to add the electromagnetic interaction to the quark action because amplitudes with different numbers of real photons must be evaluated separately, before being combined in the inclusive rate for a given process. In Ref. [1] for the first time we introduced and discussed a strategy to compute electromagnetic radiative corrections to leptonic decays of pseudoscalar mesons which can then be used to determine the corresponding CKM matrix elements. Although we present the explicit discussion for this specific set of processes, the method is more general and can readily be

extended to generic processes including, for example, to semileptonic decays.

In this talk we illustrate this strategy and present first numerical results of an exploratory calculation. These results are encouraging and make us confident that the calculation is feasible and can achieve the required precision.

2. The general strategy

We now focus on the leptonic decay of the charged pseudoscalar meson P^+. Let Γ_0 be the partial width for the decay $P^+ \to \ell^+ \nu_\ell$ where the charged lepton ℓ is an electron or a muon (or possibly a τ) and ν_ℓ is the corresponding neutrino. The subscript 0 indicates that there are no photons in the final state. In the absence of electromagnetism, the non-perturbative QCD effects are contained in a single number, the decay constant f_P, defined by

$$\langle 0 \,|\, \bar{q}_1 \gamma^\mu \gamma^5 q_2 \,|\, P^+(p) \rangle = i p^\mu f_P \,, \tag{2.1}$$

where P^+ is composed of the valence quarks $\bar{q}_1$ and q_2, and the axial current in (2.1) is composed of the corresponding quark fields. There have been very many lattice calculations of the decay constants $f_\pi, f_K, f_{D_{(s)}}$ and $f_{B_{(s)}}$ [2], some of which are approaching $O(1\%)$ precision. As noted above, in order to determine the corresponding CKM matrix elements at this level of precision isospin breaking effects, including electromagnetic corrections, must be considered. It will become clear in the following, and has been stressed in [13, 14], that it is not possible to give a physical definition of the decay constant f_P in the presence of electromagnetism, because of the contributions from diagrams in which the photon is emitted by the hadron and absorbed by the charged lepton. Thus the physical width is not just given in terms of the matrix element of the axial current and can only be obtained by a full calculation of the electromagnetic corrections at a given order.

The calculation of electromagnetic effects leads to an immediate difficulty: Γ_0 contains infrared divergences and by itself is therefore unphysical. The well-known solution to this problem is to include the contributions from real photons. We therefore define $\Gamma_1(\Delta E)$ to be the partial width for the decay $P^+ \to \ell^+ \nu_\ell \gamma$ where the energy of the photon in the rest frame of P^+ is integrated from 0 to ΔE. The sum $\Gamma_0 + \Gamma_1(\Delta E)$ is free from infrared divergences (although, of course, it does depend on the energy cut-off ΔE). We restrict the discussion to $O(\alpha)$ corrections, where α is the electromagnetic fine-structure constant, and hence only consider a single photon.

The previous paragraph reminds us that the determination of the CKM matrix elements $V_{q_1 q_2}$ at $O(\alpha)$ (i.e. at $O(1\%)$ or better) from leptonic decays requires the evaluation of amplitudes with a real photon. The main goal of this talk is to illustrate how such a calculation might be performed with non-perturbative accuracy. There are a number of technicalities which will be explained in the following sections, but here we present a general outline of the proposed method. We start with the experimental observable $\Gamma(\Delta E)$, the partial width for $P^+ \to \ell^+ \nu_\ell(\gamma)$. The final state consists either of $\ell^+ \nu_\ell$ or of $\ell^+ \nu_\ell \gamma$ where the energy of the photon in the centre-of-mass frame is smaller than ΔE:

$$\Gamma(\Delta E) = \Gamma_0 + \Gamma_1(\Delta E) \,. \tag{2.2}$$

In principle at least, $\Gamma_1(\Delta E)$ can be evaluated in lattice simulations by computing the amplitudes for a range of photon momenta and using the results to perform the integral over phase space.

Such calculations would be very challenging. Since the computations are necessarily performed in finite volumes the available momenta are discrete, so that it would be necessary to choose the volumes appropriately and compute several correlation functions. We choose instead to make use of the fact that a very soft photon couples to a charged hadron as if to an elementary particle; it does not resolve the structure of the hadron. We therefore propose to choose ΔE to be sufficiently small that the pointlike approximation can be used to calculate $\Gamma_1(\Delta E)$ in perturbation theory, treating P^+ as an elementary particle. On the other hand, ΔE must be sufficiently large that $\Gamma(\Delta E)$ can be measured experimentally. We imagine setting $\Delta E = O(10\text{-}20\,\text{MeV})$ which satisfies both requirements. From Refs. [15, 16] we learn that resolutions on the energy of the photon in the rest frame of the decaying particle of this order are experimentally accessible. In Ref. [1] we presented a discussion of the uncertainties induced by treating the meson as elementary as a function of ΔE. This discussion is based on the phenomenological analyses performed in Refs. [17, 18, 19] based on the use of chiral perturbation theory at $O(p^4)$. By analyzing separately the contribution corresponding to the approximation of a point-like pion (also frequently called *inner bremsstrahlung*) from the structure dependent part and the interference of the two, this analysis shows that for the decays $\pi \to \ell\nu\gamma$ and $K \to \ell\nu\gamma$ the interference contributions are always negligible. The structure-dependent contributions can be sizeable, because they are chirally enhanced with respect to the point-like contribution. This happens in particular for the real decay $K \to e\nu_e\gamma$. On the other hand, for $E_\gamma < 20$ MeV both structure dependent and interference contributions can be safely neglected with respect to the point-like contributions, for all leptonic decays of pions and kaons. These results are shown, quantitatively, in Fig. 1.

It is necessary to ensure that the cancellation of infrared divergences occurs with good numerical precision leading to an accurate result for $\Gamma(\Delta E)$. Since Γ_0 is to be calculated in a Monte-Carlo simulation and $\Gamma_1(\Delta E)$ in perturbation theory using the pointlike approximation, this requires an intermediate step. We propose to rewrite Eq. (2.2) in the form

$$\Gamma(\Delta E) = \lim_{V\to\infty}(\Gamma_0 - \Gamma_0^{\rm pt}) + \lim_{V\to\infty}(\Gamma_0^{\rm pt} + \Gamma_1(\Delta E))\,, \tag{2.3}$$

where V is the volume of the lattice. $\Gamma_0^{\rm pt}$ is an unphysical quantity; it is the perturbatively calculated amplitude at $O(\alpha)$ for the decay $P^+ \to \ell^+\nu_\ell$ with the P^+ treated as an elementary particle. In $\Gamma_0^{\rm pt}$ the finite-volume sum over the momenta of the photon is performed over the full range. The contributions from small momenta to Γ_0 and $\Gamma_0^{\rm pt}$ are the same and thus the infrared divergences cancel in the first term on the right-hand side of Eq. (2.3). Moreover, the infrared divergences in Γ_0 and $\Gamma_0^{\rm pt}$ are both equal and opposite to that in $\Gamma_1(\Delta E)$. The infrared divergences therefore cancel separately in each of the two terms on the right-hand side of Eq. (2.3) and indeed we treat each of these terms separately. $\Gamma_0^{\rm pt} + \Gamma_1(\Delta E)$ is calculated in perturbation theory directly in infinite volume. The QCD effects in Γ_0 are calculated stochastically in a lattice simulation and the virtual photon is included explicitly (in the Feynman gauge). For each photon momentum this is combined with $\Gamma_0^{\rm pt}$ and the difference is summed over the momenta and then the infinite-volume limit is taken. This completes the sketch of the proposed method, and in the remainder of this talk we explain the many technical issues which must be addressed.

It will be helpful in the following to define $\Delta\Gamma_0(L)$ in terms of the first term on the right-hand side of Eq. (2.3):

$$\Delta\Gamma_0(L) = \Gamma_0(L) - \Gamma_0^{\rm pt}(L)\,, \tag{2.4}$$

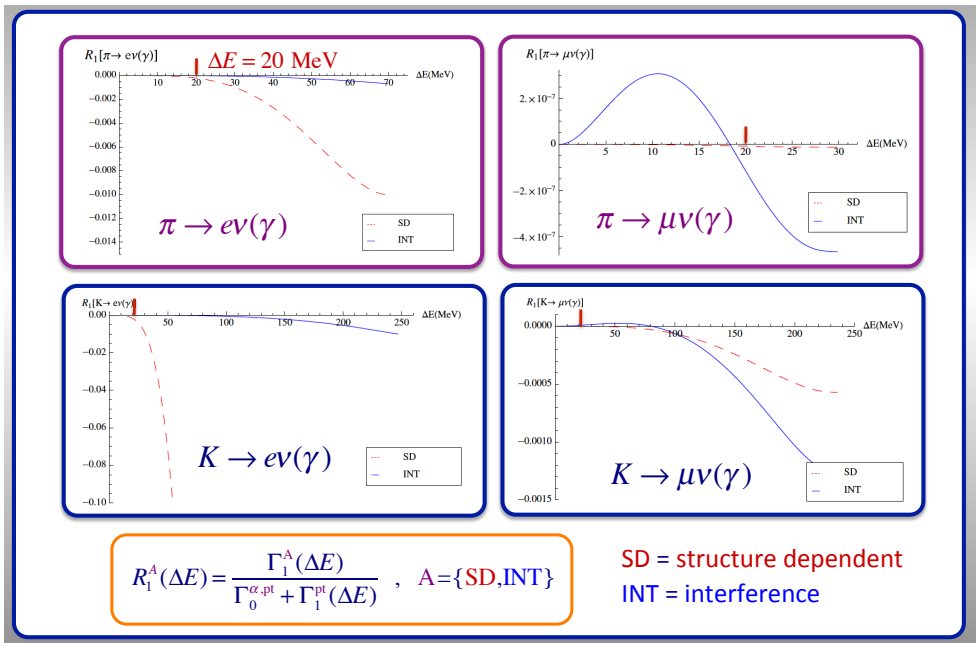

Figure 1: Ratios between the structure-dependent (SD) and interference (INT) contributions to the decay rates to the $O(\alpha)$ point-like (pt) one, for the decays $\pi \to \ell\nu\gamma$ and $K \to \ell\nu\gamma$. The estimates are obtained by using phenomenological determinations of the relevant form factors based on chiral perturbation theory at $O(p^4)$.

where we have made the dependence on the volume explicit, $V = L^3$ and L is the length of the lattice in any spacial direction (for simplicity we assume that this length is the same in all three directions). In analogy to Eq. (2.2) we also define the perturbative quantity

$$\Gamma^{\rm pt}(\Delta E) = \Gamma_0^{\rm pt} + \Gamma_1(\Delta E)\,. \tag{2.5}$$

We note that, since the sum of all the terms in Eq. (2.3) is gauge invariant as is the perturbative rate $\Gamma^{\rm pt}(\Delta E)$, the combination $\Delta\Gamma_0(L)$ is also gauge invariant, although each of the two terms is not.

In this talk we now discuss, in turn, the effective weak Hamiltonian and its renormalisation in the presence of electromagnetism, the structure of the calculation and the correlation functions which need to be calculated on the lattice, the evaluation in perturbation theory at one loop of the second term on the right-hand side of Eq. (2.3), $\Gamma^{\rm pt}(\Delta E)$. We finally put all the elements of the calculation together, present the results of a preliminary numerical investigation and conclude with a summary and presenting some future perspectives.

In the remainder of the talk, to be specific we choose $P^+ = \pi^+$ but the discussion generalizes trivially to other pseudoscalar mesons with the obvious changes of flavour labels. The method does not require P^+ to be a light psuedo-Goldstone Boson nor on the use of chiral perturbation theory.

3. Matching the effective local four-quark operator(s) onto the standard model

At lowest order in electromagnetic (and strong) perturbation theory the process $u\bar{d} \to \ell^+\nu_\ell$

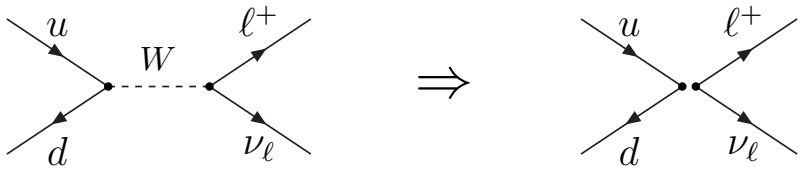

Figure 2: Tree-level diagram for the process $u\bar{d} \to \ell^+ \nu_\ell$ (left-hand diagram). In the effective theory the interaction is replaced by a local four-fermion operator (right-hand diagram).

proceeds by an s-channel W exchange, see the left-hand diagram in Fig. 2. Since the energy-momentum exchanges in this process are much smaller than M_W, it is standard practice to rewrite the amplitude in terms of a four-fermion local interaction:

$$\mathscr{L}_W = -\frac{4G_F}{\sqrt{2}} V_{ud}^* \left(\bar{d}_L \gamma_\mu u_L\right) \left(\bar{\nu}_{\ell L} \gamma^\mu \ell_L\right), \tag{3.1}$$

where the subscript L represents *left*, $\psi_L = \frac{(1-\gamma_5)}{2}\psi$, and G_F is the Fermi constant. In performing lattice computations this replacement is necessary, since the lattice spacing a is much greater than $1/M_W$, where M_W is the mass of the W-Boson. When including the $O(\alpha)$ corrections, the ultra-violet contributions to the matrix element of the local operator are different to those in the Standard Model and in this section we discuss the matching factors which must be introduced to determine the $O(\alpha)$ corrections to the $\pi^+ \to \ell^+ \nu_\ell$ decay from lattice computations of correlation functions containing the local operator in (3.1). Since the pion decay width is written in terms of G_F, it is necessary to start by revisiting the determination of the Fermi constant at $O(\alpha)$.

3.1 Determination of the Fermi constant, G_F

G_F is conventionally taken from the measured value of the muon lifetime using the expression [20, 21]

$$\frac{1}{\tau_\mu} = \frac{G_F^2 m_\mu^5}{192\pi^3}\left[1 - \frac{8m_e^2}{m_\mu^2}\right]\left[1 + \frac{\alpha}{2\pi}\left(\frac{25}{4} - \pi^2\right)\right], \tag{3.2}$$

leading to the value $G_F = 1.16634 \times 10^{-5}\,\text{GeV}^{-2}$. (For an extension of Eq. (3.2) to $O(\alpha^2)$ and the inclusion of higher powers of $\rho \equiv (m_e/m_\mu)^2$ see Sec. 10.2 of [22].)

Eq. (3.2) can be viewed as the definition of G_F. When calculating the Standard Model corrections to the muon lifetime many of the contributions are absorbed into G_F and the remaining terms on the right-hand side of (3.2) come from the diagrams in Fig. 3. Specifically in these diagrams the factor $1/k^2$ in the Feynman-gauge photon propagator is replaced by $1/k^2 \times M_W^2/(M_W^2 - k^2)$, where k is the momentum in the propagator; this is called the W-regularisation of ultra-violet divergences. These diagrams are evaluated in the effective theory with the local four-fermion operator $(\bar{\nu}_\mu \gamma^\mu (1-\gamma^5)\mu)\,(\bar{e}\gamma^\mu(1-\gamma^5)\nu_e)$.

An explanation of the reasoning behind the introduction of the W-regularisation is given in [23]. The Feynman-gauge photon propagator is rewritten as two terms:

$$\frac{1}{k^2} = \frac{1}{k^2 - M_W^2} + \frac{M_W^2}{M_W^2 - k^2}\frac{1}{k^2} \tag{3.3}$$

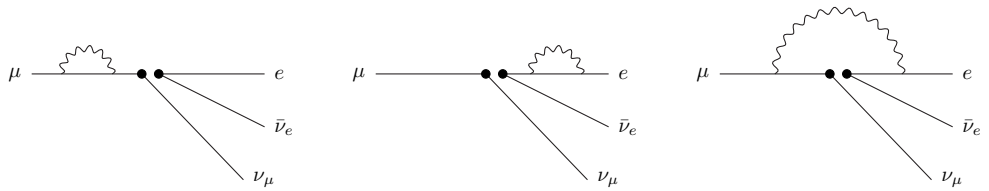

Figure 3: Diagrams contributing to the $O(\alpha)$ corrections to muon decay; see Eq. (3.2). The curly line represents the photon.

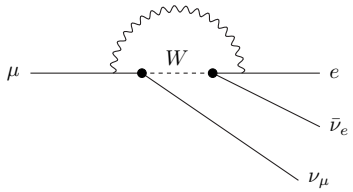

Figure 4: Photon-W box diagrams contributing to the $O(\alpha)$ corrections to muon decay in the Standard Model. The curly line represents the photon.

and the ultra-violet divergent contributions come from the first term and are absorbed in the definition of G_F. In addition, the Standard-Model γ-W box diagram in Fig. 4 is ultra-violet convergent and is equal to the corresponding diagram in the effective theory (i.e. the third diagram in Fig. 3) with the W-regularisation, up to negligible corrections of $O(q^2/M_W^2)$, where q is the four-momentum of the electron and its neutrino. Other electroweak corrections not explicitly mentioned above are all absorbed into G_F.

3.2 W-regularisation and Weak Decays of Hadrons

It is a particularly helpful feature that most of the terms which are absorbed into the definition of G_F are common to other processes, including the leptonic decays of pseudoscalar mesons [24, 25]. There are however, some short-distance contributions which do depend on the electric charges of the individual fields in the four-fermion operators and these lead to a correction factor of $(1+\frac{2\alpha}{\pi}\log\frac{M_Z}{M_W})$ to Γ_0 [24]. This is a tiny correction ($\simeq 0.06\%$), but one which nevertheless can readily be included explicitly.

The conclusion of the above discussion is that the evaluation of the amplitude for the process $\pi^+ \to \ell^+\nu$ up to $O(\alpha)$ can be performed in the effective theory with the effective Hamiltonian

$$H_{\rm eff} = \frac{G_F}{\sqrt{2}} V_{ud}^* \left(1+\frac{\alpha}{\pi}\log\frac{M_Z}{M_W}\right) (\bar{d}\gamma^\mu(1-\gamma^5)u)\,(\bar{\nu}_\ell\gamma_\mu(1-\gamma^5)\ell)\,, \tag{3.4}$$

and with the Feynman-gauge photon propagator in the W-regularisation. The value of G_F is obtained from the muon lifetime as discussed around Eq. (3.2).

Of course we are not able to implement the W-regularisation directly in present day lattice simulations in which the inverse lattice spacing is much smaller than M_W. The relation between the operator in eq. (3.4) in the lattice and W regularisations can be computed in perturbation theory.

Thus for example, with the Wilson action for both the gluons and fermions:

$$O_1^{\mathrm{W-reg}} = \left(1+\frac{\alpha}{4\pi}\left(2\log a^2M_W^2 - 15.539\right)\right) O_1^{\mathrm{bare}} + \frac{\alpha}{4\pi}\left(0.536\, O_2^{\mathrm{bare}} + 1.607\, O_3^{\mathrm{bare}} - 3.214\, O_4^{\mathrm{bare}} - 0.804\, O_5^{\mathrm{bare}}\right), \tag{3.5}$$

where

$$\begin{aligned} O_1 &= (\bar{d}\gamma^\mu(1-\gamma^5)u)\,(\bar{\nu}_\ell\gamma_\mu(1-\gamma^5)\ell) & O_2 &= (\bar{d}\gamma^\mu(1+\gamma^5)u)\,(\bar{\nu}_\ell\gamma_\mu(1-\gamma^5)\ell) \\ O_3 &= (\bar{d}(1-\gamma^5)u)\,(\bar{\nu}_\ell(1+\gamma^5)\ell) & O_4 &= (\bar{d}(1+\gamma^5)u)\,(\bar{\nu}_\ell(1+\gamma^5)\ell) \\ O_5 &= (\bar{d}\sigma^{\mu\nu}(1+\gamma^5)u)\,(\bar{\nu}_\ell\sigma_{\mu\nu}(1+\gamma^5)\ell)\,. \end{aligned} \tag{3.6}$$

The superscript “bare" indicates that these are bare operators in the lattice theory and the presence of 5 operators on the right-hand side of Eq. (3.5) is a consequence of the breaking of chiral symmetry in the Wilson theory. Using lattice actions with good chiral symmetry, such as domain wall fermions with a sufficiently large fifth dimension, only O_1^{bare} would appear on the right-hand side of Eq.(3.5). The coefficients multiplying the operators depend of course on the lattice action being used. Eq. (3.5) is valid up to corrections of $O(\alpha_s(a)\,\alpha)$.

Having formulated the problem of calculating Γ_0 in terms of the evaluation of correlation functions involving the effective Hamiltonian in Eq. (3.4) we are now in a position to discuss how the calculations of the amplitudes for the processes $\pi^+ \to \ell^+\nu$ and $\pi^+ \to \ell^+\nu\gamma$ are to be performed.

4. Calculation of $\Delta\Gamma_0(L)$

In this section we describe the lattice calculation of $\Delta\Gamma_0(L)$ at $O(\alpha)$, i.e. the first term on the right-hand side of Eq. (2.3). Before entering into the details however, we add some comments on the structure of the different terms appearing in Eq. (2.3).

Since we add and subtract the same perturbative quantity Γ_0^{pt}, we find it convenient to choose this to be the virtual decay rate for a point-like pion computed in the W-regularisation. In this way we obtain the important advantage that the difference of the first two terms ($\Delta\Gamma_0(L)$) and the sum of the last two terms ($\Gamma^{\mathrm{pt}}(\Delta E)$) on the r.h.s. of Eq. (2.3) are separately ultraviolet and infrared finite.

Let $\sqrt{Z_\ell}$ be the contribution to the decay amplitude from the electromagnetic wave-function renormalisation of the final state lepton (see the diagram in Fig. 6(d)). An important simplifying feature of this calculation is that Z_ℓ cancels in the difference $\Gamma_0 - \Gamma_0^{\mathrm{pt}}$. This is because in any scheme and using the same value of the decay constant f_π, the contribution from the diagram in Fig. 6(d) computed non-perturbatively or perturbatively with the point-like approximation are the same. Thus we only need to calculate Z_ℓ directly in infinite volume and include it in the second term on the right-hand side of Eq. (2.3).

Let us now briefly recall the calculation of Γ_0 at $O(\alpha^0)$, i.e. without electromagnetism.

4.1 Calculation of Γ_0 at $O(\alpha^0)$

Without electromagnetic corrections we need to compute the correlation function sketched in Fig. 5, which is a completely standard calculation. Since the leptonic terms are factorized from the

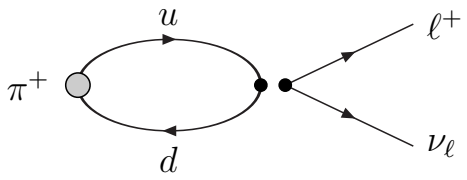

Figure 5: Correlation function used to calculate the amplitude for the leptonic decay of the pion in pure QCD. The two black filled circles represent the local current-current operator $(\bar{d}\gamma_L^\mu u)\,(\bar{\nu}_\ell\gamma_\mu\ell)$; the circles are displaced for convenience.

hadronic ones, the amplitude is simply given by

$$\begin{aligned}\bar{u}_{\nu_\ell\,\alpha}(p_{\nu_\ell})\,(M_0)_{\alpha\beta}\,v_{\ell\,\beta}(p_\ell) &= \frac{G_F}{\sqrt{2}}V_{ud}^*\,\langle 0\,|\,\bar{d}\gamma^\nu\gamma^5\,u\,|\pi^+(p_\pi)\rangle\,\left[\bar{u}_{\nu_\ell}(p_{\nu_\ell})\gamma_\nu(1-\gamma^5)\,v_\ell(p_\ell)\right]\\ &= \frac{iG_F f_\pi}{\sqrt{2}}V_{ud}^*\,p_\pi^\nu\,\left[\bar{u}_{\nu_\ell}(p_{\nu_\ell})\gamma_\nu(1-\gamma^5)\,v_\ell(p_\ell)\right]. \qquad (4.1)\end{aligned}$$

Here u,d in the matrix element represent the quark fields with the corresponding flavour quantum numbers and u_{ν_ℓ} and v_ℓ the spinors of the leptons defined by the subscript. The hadronic matrix element, and hence the decay constant f_π, are obtained in the standard way by computing the correlation function

$$C_0(t)\equiv\sum_{\vec{x}}\,\langle 0\,|\left(\bar{d}(\vec{0},0)\gamma^A\gamma^5\,u(\vec{0},0)\right)\phi^\dagger(\vec{x},-t)\,|0\rangle\simeq\frac{Z_0^\phi}{2m_\pi^0}e^{-m_\pi^0 t}\,\mathscr{A}_0\,, \qquad (4.2)$$

where $\phi^\dagger$ is an interpolating operator which can create the pion out of the vacuum, $Z_0^\phi\equiv\langle\pi^+(\vec{0})|\phi^\dagger(0,\vec{0})\,|0\rangle$ and $\mathscr{A}_0\equiv\langle 0\,|\,\bar{d}\gamma^A\gamma^5\,u\,|\pi^+(\vec{0})\rangle_0$. We have chosen to place the weak current at the origin and to create the pion at negative time $-t$, where t and $T-t$ are sufficiently large to suppress the contributions from heavier states and from the backward propagating pions (this latter condition may be convenient but is not necessary). The subscript or superscript 0 here denotes the fact that the calculation is performed at $O(\alpha^0)$, i.e. in the absence of electromagnetism. Z_0^ϕ is obtained from the two-point correlation function of two ϕ operators:

$$C_0^{\phi\phi}(t)\equiv\sum_{\vec{x}}\,\langle 0\,|T\{\phi(\vec{0},0)\,\phi^\dagger(\vec{x},-t)\}\,|0\rangle\simeq\frac{(Z_0^\phi)^2}{2m_\pi^0}\,e^{-m_\pi^0 t}\,. \qquad (4.3)$$

For convenience we take ϕ to be a local operator (e.g. at $(\vec{x},-t)$ in Eq. (4.2)), but this is not necessary for our discussion. Any interpolating operator for the pion on the chosen time slice would do equally well.

Having determined $\mathscr{A}_0$ and hence the amplitude $\bar{u}_{\nu_\ell\,\alpha}(p_{\nu_\ell})(M_0)_{\alpha\beta}\,v_{\ell\,\beta}(p_\ell)$, the $O(\alpha^0)$ contribution to the decay width is readily obtained

$$\Gamma_0^{\rm tree}(\pi^+\to\ell^+\nu_\ell)=\frac{G_F^2\,|V_{ud}|^2 f_\pi^2}{8\pi}\,m_\pi\,m_\ell^2\left(1-\frac{m_\ell^2}{m_\pi^2}\right)^2. \qquad (4.4)$$

In this equation we use the label tree to denote the absence of electromagnetic effects since the subscript 0 here indicates that there are no photons in the final state.

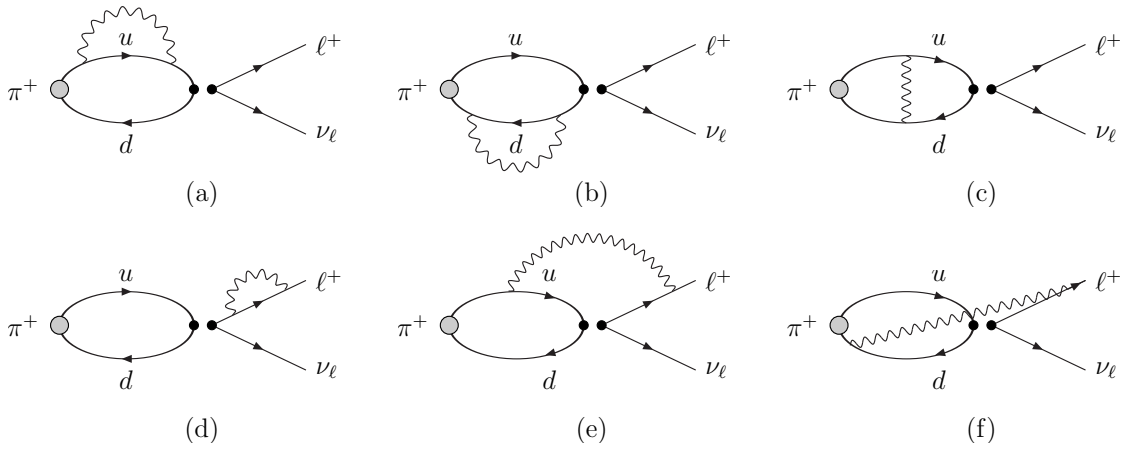

Figure 6: Connected diagrams contributing at $O(\alpha)$ contribution to the amplitude for the decay $\pi^+ \to \ell^+ \nu_l$.

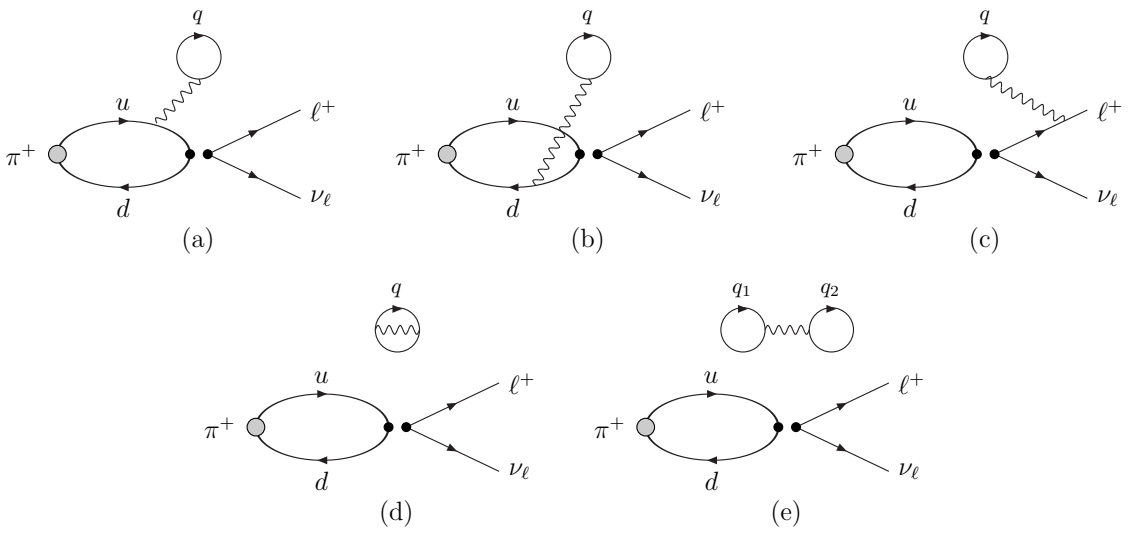

Figure 7: Disconnected diagrams contributing at $O(\alpha)$ contribution to the amplitude for the decay $\pi^+ \to \ell^+ \nu_l$. The curly line represents the photon and a sum over quark flavours q, q_1 and q_2 is to be performed.

4.2 Calculation at $O(\alpha)$

We now consider the one-photon exchange contributions to the decay $\pi^+ \to \ell^+ \nu_\ell$ and show the corresponding six connected diagrams in Fig. 6 and the disconnected diagrams in Fig. 7. By "disconnected" here we mean that there is a sea-quark loop connected, as usual, to the remainder of the diagram by a photon and/or gluons (the presence of the gluons is implicit in the diagrams). The photon propagator in these diagrams in the Feynman gauge and in infinite (Euclidean) volume is given by

$$\delta_{\mu\nu}\Delta(x_1,x_2) = \delta_{\mu\nu}\int \frac{d^4k}{(2\pi)^4}\,\frac{e^{ik\cdot(x_1-x_2)}}{k^2}\,. \tag{4.5}$$

In a finite volume the momentum integration is replaced by a summation over the momenta

which are allowed by the boundary conditions. For periodic boundary conditions, we can neglect the contributions from the zero-mode $k = 0$ since a very soft photon does not resolve the structure of the pion and its effects cancel in $\Gamma_0 - \Gamma_0^{\rm pt}$ in Eq. (2.3). For this reason in the following Γ_0 and $\Gamma_0^{\rm pt}$ are evaluated separately but using the following expression for the photon propagator in finite volume:

$$\delta_{\mu\nu}\Delta(x_1,x_2) = \delta_{\mu\nu}\,\frac{1}{L^4}\sum_{k=\frac{2\pi}{L}n;k\neq 0}\frac{e^{ik\cdot(x_1-x_2)}}{4\sum_\rho \sin^2\frac{k_\rho}{2}}\,, \tag{4.6}$$

where all quantities are in lattice units and the expression corresponds to the simplest lattice discretisation. k, n, x_1 and x_2 are four component vectors and for illustration we have taken the temporal and spatial extents of the lattice to be the same (L).

For other quantities, the presence of zero momentum excitations of the photon field is a subtle issue that has to be handled with some care. In the case of the hadron spectrum the problem has been studied in [26] and, more recently in [4, 5], where it has been shown, at $O(\alpha)$, that the quenching of zero momentum modes corresponds in the infinite-volume limit to the removal of sets of measure zero from the functional integral and that finite volume effects are different for the different prescriptions.

We now divide the discussion of the diagrams in Fig. 6 and Fig. 7 into three classes: those in which the photon is attached at both ends to the quarks (diagrams 6(a)-6(c) and 7(a), (b), (d) and (e)), those in which the photon propagates between one of the quarks and the outgoing lepton (diagrams 6(e), 6(f) and 7(c)) and finally diagram 6(d) which corresponds to the mass and wave-function normalisation of the charged lepton. We have already observed that the wave function renormalisation of the lepton cancels in the difference $\Gamma_0 - \Gamma_0^{\rm pt}$ in Eq. (2.3), so we now turn to the remaining diagrams.

• *The evaluation of diagrams Fig. 6(a)-(c) and Fig. 7(a),(b) and (d)*: We start by considering the connected diagrams 6(a)-(c). For these diagrams, the leptonic contribution to the amplitude is contained in the factor $\left[\bar{u}_{\nu_\ell}(p_{\nu_\ell})\gamma^\nu(1-\gamma^5)\,v_\ell(p_\ell)\right]$ and we need to compute the Euclidean hadronic correlation function

$$C_1(t) = -\frac{1}{2}\int d^3\vec{x}\,d^4x_1\,d^4x_2\;\langle 0|T\left\{J_W^\nu(0)\,j_\mu(x_1)\,j_\mu(x_2)\phi^\dagger(\vec{x},-t)\right\}|0\rangle\;\Delta(x_1,x_2)\,. \tag{4.7}$$

where T represents time-ordering, J_W^ν is the V–A current $\bar{d}\gamma^\nu(1-\gamma^5)\,u$ and we take $-t<0$. j_μ is the hadronic component of the electromagnetic current and we find it convenient to include the charges of the quarks Q_f in the definition of j:

$$j_\mu(x) = \sum_f Q_f\,\bar{f}(x)\gamma_\mu f(x)\,, \tag{4.8}$$

where the sum is over all quark flavours f. The factor of $1/2$ is the standard combinatorial one.

The computations are performed in Euclidean space and in a finite-volume with the photon propagator Δ given in Eq. (4.6) (or the corresponding expression for other lattice discretisations). The absence of the zero mode in the photon propagator implies a gap between m_π and the energies of the other eigenstates. Provided one can separate the contributions of these heavier states from that of the pion, one can perform the continuation of the correlation function in Eq. (4.7) from

Minkowski to Euclidean space without encountering any singularities. From the correlation function $C_1(t)$ we obtain the electromagnetic shift in the mass of the pion and also a contribution to the physical decay amplitude, as we now explain. For sufficiently large t the correlation function is dominated by the ground state, i.e. the pion, and we have

$$C_0(t)+C_1(t) \simeq \frac{e^{-m_\pi t}}{2m_\pi} Z^\phi \langle 0|J_W^0(0)|\pi^+\rangle , \tag{4.9}$$

where the electromagnetic terms are included in all factors (up to $O(\alpha)$). Writing $m_\pi = m_\pi^0 + \delta m_\pi$, where δm_π is the $O(\alpha)$ mass shift,

$$e^{-m_\pi t} \simeq e^{-m_\pi^0 t}(1-\delta m_\pi t) \tag{4.10}$$

so that $C_1(t)$ is of the schematic form

$$C_1(t) = C_0(t)(c_1 t + c_2) . \tag{4.11}$$

By determining c_1 we obtain the electromagnetic mass shift, $\delta m_\pi = -c_1$, and from c_2 we obtain the electromagnetic correction to $Z^\phi \langle 0|J_W(0)|\pi^+\rangle/2m_\pi$. Note that δm_π is gauge invariant and infrared finite, whereas the coefficient c_2 obtained from these diagrams is neither.

In order to obtain the contribution to the $\pi \to \ell\nu_\ell$ decay amplitude $\mathscr{A}$ we need to remove the factor $(e^{-m_\pi t}/2m_\pi)Z^\phi$ on the right-hand side of Eq. (4.9), including the $O(\alpha)$ corrections to this factor. Having determined c_1, we are in a position to subtract the corrections present in m_π. The $O(\alpha)$ corrections to Z^ϕ are determined in the standard way, by performing the corresponding calculation to $C_1(t)$ but with the axial current A replaced by ϕ:

$$C_1^{\phi\phi}(t) = -\frac{1}{2}\int d^3\vec{x}\, d^4x_1\, d^4x_2\, \langle 0|T\left\{\phi(\vec{0},0)\, j_\mu(x_1) j_\mu(x_2)\phi^\dagger(\vec{x},t)\right\}|0\rangle \Delta(x_1,x_2) \tag{4.12}$$

$$= C_0^{\phi\phi}(t)(c_1 t + c_2^{\phi\phi}) . \tag{4.13}$$

We finally obtain

$$Z^\phi = Z_0^\phi \left(1+\frac{1}{2}\left(c_2^{\phi\phi} - \frac{c_1}{m_\pi^0}\right)\right) , \tag{4.14}$$

and the $O(\alpha)$ contribution to the amplitude from these three diagrams is

$$\delta\mathscr{A} = \mathscr{A}_0\left(c_2 - \frac{c_2^{\phi\phi}}{2} - \frac{c_1}{2m_\pi^0}\right) . \tag{4.15}$$

For these three diagrams the $O(\alpha)$ term can be simply considered as a correction to f_π. Note however, that such an "f_π" would not be a physical quantity as it contains infrared divergences.

The treatment of the disconnected diagrams in Figs. 7(a), (b), (d) and (e) follows in exactly the same way. These diagrams contribute to the electromagnetic corrections to both the pion mass and the decay amplitude in an analogous way to the discussion of the connected diagrams above. It is standard and straightforward to write down the corresponding correlation functions in terms of quark propagators. We do not discuss here the different possibilities for generating the necessary quark propagators to evaluate the diagrams; for example we can imagine using sequential propagators or some techniques to generate all-to-all quark propagators.

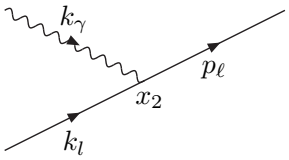

Figure 8: Zoom of the lepton-photon vertex at x_2 from the diagrams in Fig. 6(e) and (f).

• *The evaluation of diagrams Fig. 6(e)-(f)*: For these diagrams the leptonic and hadronic contributions do not factorise and indeed the contribution cannot be written simply in terms of the parameter f_π. We start by considering the Minkowski space quantity

$$\bar{u}_{\nu_\ell\,\alpha}(p_{\nu_\ell})(\bar{M}_1)_{\alpha\beta}\,v_{\ell\,\beta}(p_\ell) \;=\; -\int d^4x_1\,d^4x_2\,\langle 0|\,T\big(j_\mu(x_1)J_W^\nu(0)\big)\,|\pi\rangle \\ \times iD_M(x_1,x_2)\big\{\bar{u}_{\nu_\ell}(p_{\nu_\ell})\gamma^\nu(1-\gamma^5)(iS_M(x_2))\gamma^\mu v_\ell(p_\ell)\big\}e^{ip_\ell\cdot x_2}\,, \tag{4.16}$$

where iS_M and iD_M are the lepton and (Feynman gauge) photon propagators respectively in Minkowski space (more precisely the photon propagator with Lorentz indices (ρ,σ) is $iD_M g_{\rho\sigma}$, but the Lorentz indices have been contracted with the electromagnetic currents in (4.16)). In order to demonstrate that we can obtain the $O(\alpha)$ corrections to the decay amplitude from a Euclidean space correlation function, we use the reduction formula to rewrite the expression in Eq. (4.16) as

$$\bar{u}_{\nu_\ell\,\alpha}(p_{\nu_\ell})(\bar{M}_1)_{\alpha\beta}\,v_{\ell\,\beta}(p_\ell) = i\lim_{k_0\to m_\pi}(k_0{}^2-m_\pi^2)\int d^4x_1\,d^4x_2\,d^4x\,e^{-ik^0x^0} \\ \langle 0|T\big(j_\mu(x_1)J_W^\nu(0)\pi(x)\big)|0\rangle\,iD_M(x_1,x_2)\big[\bar{u}_{\nu_\ell}(p_{\nu_\ell})\gamma_\nu(1-\gamma^5)(iS_M(x_2))\gamma^\mu v_\ell(p_\ell)\big]e^{ip_\ell\cdot x_2}\,, \tag{4.17}$$

where $\pi(x)$ is the field which creates a pion with amplitude 1. On the other hand the Euclidean space correlation function which we propose to compute is

$$\bar{C}_1(t)_{\alpha\beta} \;=\; -\int d^3\vec{x}\,d^4x_1\,d^4x_2\;\langle 0|T\big\{J_W^\nu(0)\,j_\mu(x_1)\phi^\dagger(\vec{x},-t)\big\}|0\rangle\;\Delta(x_1,x_2) \\ \times\big(\gamma_\nu(1-\gamma^5)S(0,x_2)\gamma_\mu\big)_{\alpha\beta}\,e^{E_\ell t_2}e^{-i\vec{p}_\ell\cdot\vec{x}_2}. \tag{4.18}$$

Here S and Δ are Euclidean propagators, and α,β are spinor indices. As for $C_0(t)$ and $C_1(t)$, provided that the pion is the lightest hadronic state then for large t, $\bar{C}_1(t)$ is dominated by the matrix element with a single pion in the initial state.

In view of the factor $e^{E_\ell t_2}$ on the right-hand side of Eq. (4.18), the new feature in the evaluation of the diagrams in Fig. 6 (e) and (f) is that we need to ensure that the t_2 integration converges as $|t_2|\to\infty$. For $t_2<0$ the convergence of the integral is improved by the presence of the exponential factor and so we limit the discussion to the case $t_2\to\infty$. $E_\ell=\sqrt{m_\ell^2+\vec{p}_\ell{}^2}$ is the energy of the outgoing charged lepton with three-momentum $\vec{p}_\ell$. To determine the $t_2\to\infty$ behaviour, consider the lepton-photon vertex at x_2 from the diagrams in Fig. 6(e) and (f), redrawn in Fig. 8. k_ℓ and k_γ are the four-momentum variables in the Fourier transform of the propagators $S(x_2)$ and $\Delta(x_1,x_2)$ respectively in Eqs. (4.16) - (4.18). The t_2 integration is indeed convergent as we now show explicitly.

1. The integration over $\vec{x}_2$ implies three-momentum conservation at this vertex so that in the sum

over the momenta $\vec{k}_\ell + \vec{k}_\gamma = \vec{p}_l$, where p_ℓ is the momentum of the outgoing charged lepton.
2. The integrations over the energies $k_{4\,\ell}$ and $k_{4\,\gamma}$ lead to the exponential factor $e^{-(\omega_\ell+\omega_\gamma)t_2}$, where $\omega_\ell = \sqrt{\vec{k}_\ell^{\,2} + m_\ell^2}$, $\omega_\gamma = \sqrt{\vec{k}_\gamma^{\,2} + m_\gamma^2}$, and m_γ is the mass of the photon introduced as an infra-red cut-off. The large t_2 behaviour is therefore given by the factor $e^{-(\omega_\ell+\omega_\gamma-E_\ell)t_2}$.
3. A simple kinematical exercise shows that in the sum over $\vec{k}_\gamma$ (with $\vec{k}_\ell = \vec{p}_\ell - \vec{k}_\gamma$), the minimum value of $\omega_\ell + \omega_\gamma$ is given by

$$(\omega_\ell + \omega_\gamma)_{\rm min} = \sqrt{(m_\ell + m_\gamma)^2 + \vec{p}_\ell^{\,2}}\,. \tag{4.19}$$

4. Thus for non-zero m_γ, the exponent in $e^{-(\omega_\ell+\omega_\gamma-E_\ell)t_2}$ for large t_2 is negative for every term in the summation over k_γ and the integral over t_2 is convergent so that the continuation from Minkowski to Euclidean space can be performed.
5. We note that the integration over t_2 is also convergent if we set $m_\gamma = 0$ but remove the $\vec{k} = 0$ mode in finite volume. In this case $\omega_\ell + \omega_\gamma > E_l + [1 - (p_\ell/E_\ell)]|\vec{k}_{\rm min}|$.

In summary the t_2 integration is convergent because for every term in the sum over momenta $\omega_\ell + \omega_\gamma > E_l$ and so for sufficiently large t we can write

$$\bar{C}_1(t)_{\alpha\beta} \simeq Z_0^\phi \, \frac{e^{-m_\pi^0 t}}{2m_\pi^0} \, (\bar{M}_1)_{\alpha\beta} \tag{4.20}$$

and the contribution from the diagrams of Fig. 6(e) and 6(f) is $\bar{u}_\alpha(p_{\nu_\ell})(\bar{M}_1)_{\alpha\beta} v_\beta(p_\ell)$. This completes the demonstration that the Minkowski-space amplitude (4.17) is equal to the pion contribution to the Euclidean correlation function (4.18), up to a factor Z_0^ϕ which accounts for the normalisation of the pion field.

Again the evaluation of the correction to the amplitude from the disconnected diagram in Fig. 7(c) follows in an analogous way.

In Fig. 9 we present preliminary results of an exploratory numerical calculation of the diagrams of Fig. 6(e)-(f). We used the gauge configurations produced by the ETM Collaboration with twisted mass fermions and $N_f = 2$ dynamical flavors [27][1]. The results have been obtained by averaging over 240 gauge field configurations, with 4 stochastic sources per configuration, on a $24^3 \times 48$ lattice with lattice spacing of about 0.086 fm. The mass of the decaying pseudoscalar meson (kaon or pion) is about 475 MeV. The largest contributions to the amplitude exhibit a statistical precision at the level of 1% or better. This makes us very confident that the lattice calculation of QED corrections to the leptonic decay, though challenging, is feasible and can reach the accuracy required by phenomenology.

5. Calculation of $\Gamma^{\rm pt}(\Delta E)$

In this section we describe the calculation of the second term of Eq. (2.3), $\Gamma^{\rm pt}(\Delta E) = \Gamma_0^{\rm pt} + \Gamma_1(\Delta E)$ at $O(\alpha)$.

The evaluation in perturbation theory of the total width $\Gamma^{\rm pt} = \Gamma_0^{\rm pt} + \Gamma_1^{\rm pt}$ in infinite volume, was performed by Berman and Kinoshita in 1958/9 [20, 28], using the Pauli-Villars regulator for the

[1] We thank Francesco Sanfilippo and Silvano Simula for their collaboration in producing these numerical results.

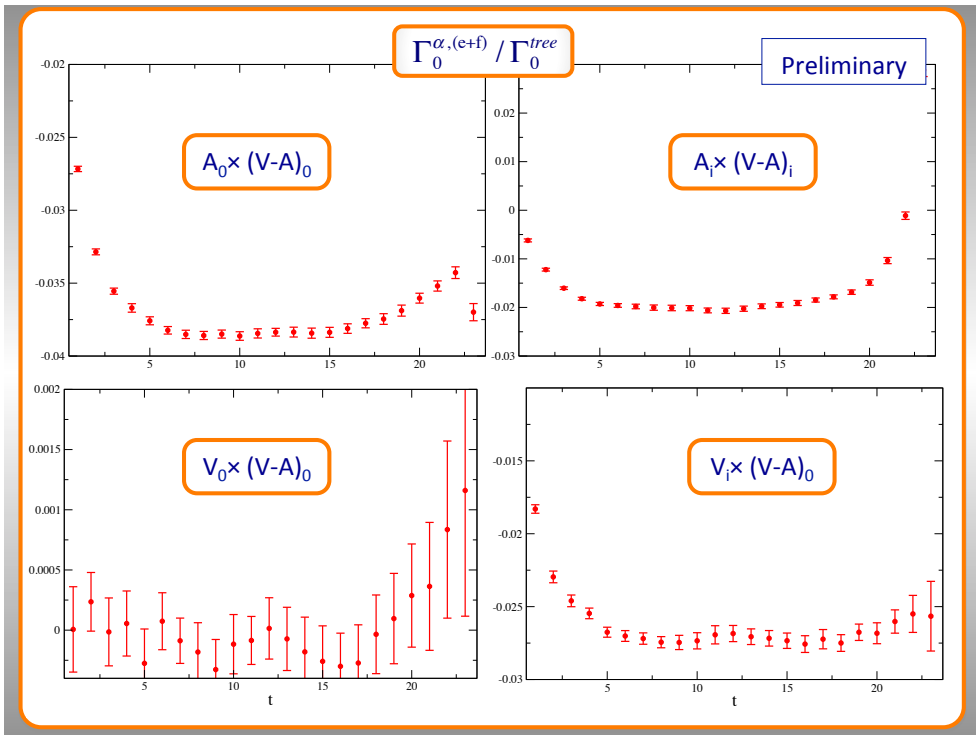

Figure 9: Preliminary lattice results for the contributions of the crossed diagrams of Fig. 6(e)-(f) to the decay rate normalized with the decay rate at tree level.

ultraviolet divergences and a photon mass to regulate the infrared divergences in both $\Gamma_0^{\rm pt}$ and $\Gamma_1^{\rm pt}$. $\Gamma_1^{\rm pt}$ is the rate for process $\pi^+ \to \ell^+ \nu_\ell \gamma$ for a pointlike pion with the energy of the photon integrated over the full kinematic range. We have added the label pt in $\Gamma_1^{\rm pt}$ to remind us that the integration includes contributions from regions of phase space in which the photon is not sufficiently soft for the structure of the pion to be reliably neglected. We do not include this label when writing $\Gamma_1(\Delta E)$ because we envisage that ΔE is sufficiently small so that the pointlike approximation reproduces the full calculation.

In our calculation, $\Gamma_0^{\rm pt}$ is evaluated in the W-regularisation, so that the ultra-violet divergences are replaced by logarithms of M_W. For convenience we write here the expression for $\Gamma^{\rm pt}(\Delta E)$ as

$$\Gamma^{\rm pt}(\Delta E) = \Gamma_0^{\rm pt} + \Gamma_1(\Delta E) = \Gamma_0^{\rm tree} + \Gamma_0^{\alpha,{\rm pt}} + \Gamma_1(\Delta E)\,. \tag{5.1}$$

$\Gamma_0^{\rm tree}$ has already been presented in Eq. (4.4). In the following we give separately the results of the remaining contributions to $\Gamma^{\rm pt}(\Delta E)$ also using a photon mass m_γ as the infrared regulator. We neglect powers of m_γ in all the results.

In the perturbative calculation we use the following Lagrangian for the interaction of a point-like pion with the leptons:

$$\mathscr{L}_{\pi-\ell-\nu_\ell} = i G_F f_\pi V_{ud}^* \left\{(\partial_\mu - ieA_\mu)\pi\right\} \left\{\bar\psi_{\nu_\ell} \frac{1+\gamma_5}{2} \gamma^\mu \psi_\ell\right\} + \text{Hermitian conjugate}\,. \tag{5.2}$$

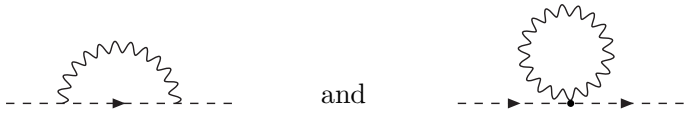

Figure 10: One loop diagrams contributing to the wave-function renormalisation of a point-like pion.

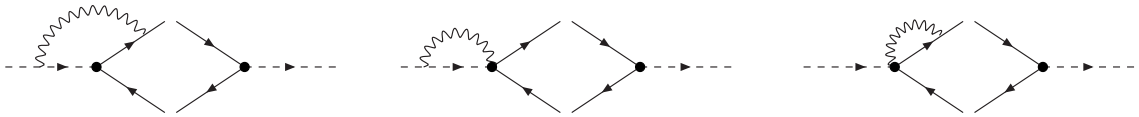

Figure 11: Radiative corrections to the pion-lepton vertex. The diagrams represent $O(\alpha)$ contributions to $\Gamma_0^{\rm pt}$. The left part of each diagram represents a contribution to the amplitude and the right part the tree-level contribution to the hermitian conjugate of the amplitude. The corresponding diagrams containing the radiative correction on the right-hand side of each diagram are also included.

The corresponding Feynman rules are:

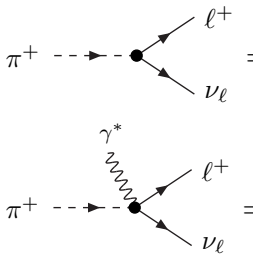

(5.3)

In addition we have used the standard Feynman rules of scalar electromagnetism for the interactions of charged pions in an electromagnetic field.

• *Wave function renormalisation of the lepton*: As already observed, provided that one uses the same value of the decay constant f_π, the contribution of the lepton wave function renormalisation to $\Gamma_0^{\alpha,{\rm pt}}$ is the same for the point-like or composite case, the latter corresponding to the diagram in Fig. 6(d). This contribution is given by

$$\Gamma_0^\ell = \Gamma_0^{\rm tree} \times \frac{\alpha}{4\pi} Z_\ell \,, \quad \text{where} \quad Z_\ell = \log\left(\frac{m_\ell^2}{M_W^2}\right) - 2\log\left(\frac{m_\gamma^2}{m_\ell^2}\right) - \frac{9}{2} \,. \tag{5.4}$$

We start by giving the $O(\alpha)$ contributions to $\Gamma_0^{\alpha,{\rm pt}}$. • *Wave function renormalisation of the pion*: The contribution of the pion wave function renormalisation to $\Gamma_0^{\alpha,{\rm pt}}$ is obtained from the diagrams in Fig. 10 and is given by

$$\Gamma_0^\pi = \Gamma_0^{\rm tree} \times \frac{\alpha}{4\pi} Z_\pi \,, \quad \text{where} \quad Z_\pi = -2\log\left(\frac{m_\pi^2}{M_W^2}\right) - 2\log\left(\frac{m_\gamma^2}{m_\pi^2}\right) - \frac{3}{2} \,. \tag{5.5}$$

These diagrams correspond to those in Fig. 6(a), Fig. 6(b) and Fig. 6(c) in the composite case.

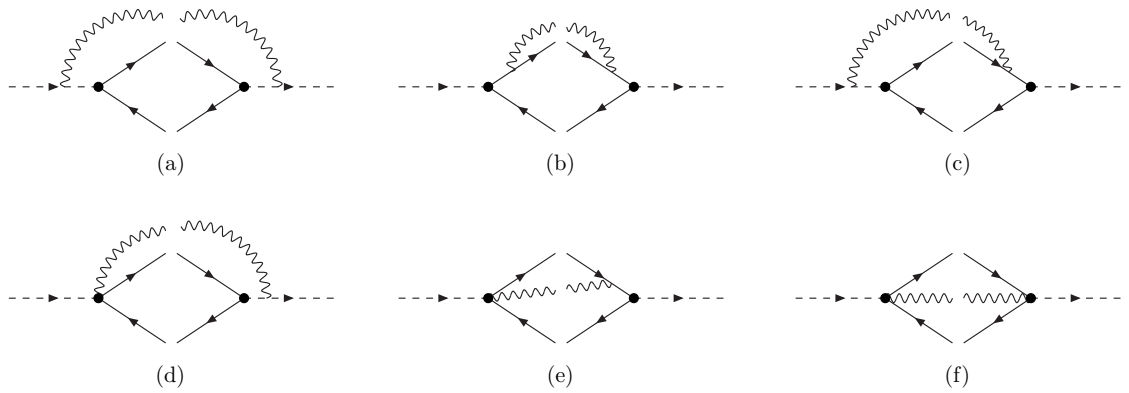

Figure 12: Diagrams contributing to $\Gamma_1(\Delta E)$. For diagrams (c), (d) and (e) the "conjugate" contributions in which the photon vertices on the left and right of each diagram are interchanged are also to be included.

• π - ℓ *Vertex*: The remaining graphs contributing to $\Gamma_0^{\alpha,\mathrm{pt}}$ are the π - ℓ vertex corrections from the diagrams shown in Fig. 11 and their complex conjugates. The contribution from these diagrams is

$$\Gamma_0^{\pi-\ell} = \Gamma_0^{\mathrm{tree}} \times \frac{\alpha}{4\pi}\left[4\log\left(\frac{m_\pi^2}{M_W^2}\right) - 2\frac{1+r_\ell^2}{1-r_\ell^2}\log\left(r_\ell^2\right)\log\left(\frac{m_\gamma^2}{m_\pi^2}\right) + \frac{1+r_\ell^2}{1-r_\ell^2}\log^2\left(r_\ell^2\right) + 2\frac{1-3r_\ell^2}{1-r_\ell^2}\log\left(r_\ell^2\right) - 1\right], \tag{5.6}$$

where $r_\ell = m_\ell/m_\pi$. These diagrams correspond to the diagrams Fig. 6(e) and Fig. 6(f) in the composite pion case.

By adding together the contributions from Eqs. (5.4) – (5.6), one obtains the complete $O(\alpha)$ contribution to the rate Γ_0^{pt},

$$\Gamma_0^{\alpha,\mathrm{pt}} = \Gamma_0^{\mathrm{tree}} \times \frac{\alpha}{4\pi}\left[3\log\left(\frac{m_\pi^2}{M_W^2}\right) - \left(4 + 2\frac{1+r_\ell^2}{1-r_\ell^2}\log\left(r_\ell^2\right)\right)\log\left(\frac{m_\gamma^2}{m_\pi^2}\right) + \frac{1+r_\ell^2}{1-r_\ell^2}\log^2\left(r_\ell^2\right) + \frac{5-9r_\ell^2}{1-r_\ell^2}\log\left(r_\ell^2\right) - 7\right], \tag{5.7}$$

Next we give the result for $\Gamma_1(\Delta E)$. This rate receives the contribution from the emission and absorption of a real photon from the pion, represented by diagram (a) in Fig. 12, from the charged lepton, represented by the diagram (b) in Fig. 12, and finally from the emission of a real photon from the pion and its absorption by the charged lepton, represented by the diagrams (c) – (f) in

Fig. 12. The result is

$$\Gamma_1(\Delta E) = \Gamma_0^{\rm tree} \times \frac{\alpha}{4\pi}\left[\left(4+2\frac{1+r_\ell^2}{1-r_\ell^2}\log\left(r_\ell^2\right)\right)\log\left(\frac{m_\gamma^2}{m_\pi^2}\right) - \frac{1+r_\ell^2}{1-r_\ell^2}\log^2\left(r_\ell^2\right) - 2\frac{1+r_\ell^2}{1-r_\ell^2}\log(r_\ell^2)\right.$$
$$-4\log(r_E^2) - 2\frac{1+r_\ell^2}{1-r_\ell^2}\log(r_E^2)\log(r_\ell^2) - 4\frac{1+r_\ell^2}{1-r_\ell^2}\,{\rm Li}_2(1-r_\ell^2) + 4$$
$$+\frac{3+r_E^2-6r_\ell^2-4r_E(1-r_\ell^2)}{(1-r_\ell^2)^2}\log(1-r_E) + \frac{r_E(4-r_E-4r_\ell^2)}{(1-r_\ell^2)^2}\log(r_\ell^2)$$
$$\left.-\frac{r_E(-22+3r_E+28r_\ell^2)}{2(1-r_\ell^2)^2} - 4\frac{1+r_\ell^2}{1-r_\ell^2}\,{\rm Li}_2(r_E)\right], \tag{5.8}$$

where $r_E = 2\Delta E/m_\pi$.

We are finally in a position to combine the results in Eqs. (5.7) and (5.8) in order to obtain the final expression for $\Gamma^{\rm pt}(\Delta E)$. As expected the infrared cutoff cancels and we find

$$\Gamma^{\rm pt}(\Delta E) = \Gamma_0^{\rm tree} \times \left(1+\frac{\alpha}{4\pi}\left\{3\log\left(\frac{m_\pi^2}{M_W^2}\right) + \frac{3-11r_\ell^2}{1-r_\ell^2}\log(r_\ell^2) - 4\log(r_E^2)\right.\right.$$
$$-2\frac{1+r_\ell^2}{1-r_\ell^2}\log(r_E^2)\log(r_\ell^2) - 4\frac{1+r_\ell^2}{1-r_\ell^2}\,{\rm Li}_2(1-r_\ell^2) - 3$$
$$+\left[\frac{3+r_E^2-6r_\ell^2-4r_E(1-r_\ell^2)}{(1-r_\ell^2)^2}\log(1-r_E) + \frac{r_E(4-r_E-4r_\ell^2)}{(1-r_\ell^2)^2}\log(r_\ell^2)\right.$$
$$\left.\left.\left.-\frac{r_E(-22+3r_E+28r_\ell^2)}{2(1-r_\ell^2)^2} - 4\frac{1+r_\ell^2}{1-r_\ell^2}\,{\rm Li}_2(r_E)\right]\right\}\right). \tag{5.9}$$

Note that the terms in square brackets in eq. (5.9) vanish when r_E goes to zero; in this limit $\Gamma^{\rm pt}(\Delta E)$ is given by its eikonal approximation.

The total rate is readily computed by setting r_E to its maximum value, namely $r_E = 1-r_\ell^2$, giving

$$\Gamma^{\rm pt} = \Gamma_0^{\rm tree} \times \left\{1+\frac{\alpha}{4\pi}\left(3\log\left(\frac{m_\pi^2}{M_W^2}\right) - 8\log(1-r_\ell^2) - \frac{3r_\ell^4}{(1-r_\ell^2)^2}\log(r_\ell^2)\right.\right. \tag{5.10}$$
$$\left.\left.-8\frac{1+r_\ell^2}{1-r_\ell^2}\,{\rm Li}_2(1-r_\ell^2) + \frac{13-19r_\ell^2}{2(1-r_\ell^2)} + \frac{6-14r_\ell^2-4(1+r_\ell^2)\log(1-r_\ell^2)}{1-r_\ell^2}\log(r_\ell^2)\right)\right\}.$$

The result in Eq. (5.10) agrees with the well known results in literature [20, 21], which provides an important check of our calculation. We believe that the result in Eq. (5.9) is new.

6. Summary and Prospects

Lattice calculations of some hadronic quantities are already approaching (or even reaching) $O(1\%)$ precision and we can confidently expect that the uncertainties will continue to be reduced

in future simulations. At this level of precision, isospin-breaking effects, including electromagnetic corrections, must be included in the determination of the relevant physical quantities. In this talk we have presented a method to compute, for the first time, electromagnetic effects in hadronic processes. For these quantities the presence of infrared divergences in the intermediate stages of the calculation makes the procedure much more complicated than is the case for the hadronic spectrum, for which calculations in several different approaches [4, 6, 5, 7, 8, 9] already exist. In order to obtain physical decay widths (or cross sections) diagrams containing virtual photons must be combined with those corresponding to the emission of real photons. Only in this way are the infrared divergences cancelled. We stress that it is not sufficient simply to add the electromagnetic interaction to the quark action because, for any given process, the contributions corresponding to different numbers of real photons must be evaluated separately.

We have discussed in detail a specific case, namely the $O(\alpha)$ radiative corrections to the leptonic decay of charged pseudoscalar mesons. The method can however, be extended to many other processes, for example to semileptonic decays. The condition for the applicability of our strategy is that there is a mass gap between the decaying particle and the intermediate states generated by the emission of the photon, so that all of these states have higher energies than the mass of the initial hadron (in the rest frame of the initial hadron).

In this talk, as in Ref. [1], we have limited the discussion to real photons with energies which are much smaller than the QCD scale $\Lambda_{\rm QCD}$. This is not a limitation of our method and in the future one can envisage numerical simulations of contributions to the inclusive width from the emission of real photons with energies which do resolve the structure of the initial hadron. Such calculations can be performed in Euclidean space under the same conditions as above, i.e. providing that there is a mass gap.

In the calculation of electromagnetic corrections a general issue concerns finite-size effects. In this respect, our method reduces to the calculation of infrared-finite, gauge-invariant quantities for which we expect the finite-size corrections to be comparable to those encountered in the computation of the spectrum. This expectation will be checked in forthcoming numerical studies and studied theoretically in chiral perturbation theory.

Although the implementation of our method is challenging, it is within reach of present lattice technology particularly as the relative precision necessary to make the results phenomenologically interesting is not exceedingly high. Since the effects we are calculating are, in general, of $O(1\%)$, calculating the electromagnetic corrections to a precision of 20% or so would already be more than sufficient. As the techniques improve and computational resources increase, the determination of both the QCD and QED effects will become even more precise. We now look forward to implementing the method described in this talk in an actual numerical simulation. The results of an exploratory calculation, which have been presented in this talk, are very promising.

Acknowledgements

Vittorio Lubicz is grateful to Michele Viviani, Laura Marcucci and the Organizing Committee of Chiral Dynamics 2015 for having been invited to present this talk and for the pleasant, stimulating and enjoyable atmosphere they succeeded in creating at this conference.

References

[1] N. Carrasco, V. Lubicz, G. Martinelli, C. T. Sachrajda, N. Tantalo, C. Tarantino and M. Testa, Phys. Rev. D **91** (2015) 7, 074506 [arXiv:1502.00257 [hep-lat]].

[2] S. Aoki, Y. Aoki, C. Bernard, T. Blum, G. Colangelo, M. Della Morte, S. Dürr and A. X. El Khadra *et al.*, Eur. Phys. J. C **74** (2014) 9, 2890 [arXiv:1310.8555 [hep-lat]].

[3] A. Duncan, E. Eichten and H. Thacker, Phys. Rev. Lett. **76** (1996) 3894 [hep-lat/9602005].

[4] S. Borsanyi *et al.*, Science **347** (2015) 1452 [arXiv:1406.4088 [hep-lat]].

[5] S. Basak *et al.* [MILC Collaboration], PoS LATTICE **2014** (2014) 116 [arXiv:1409.7139 [hep-lat]].

[6] G. M. de Divitiis, R. Frezzotti, V. Lubicz, G. Martinelli, R. Petronzio, G. C. Rossi, F. Sanfilippo and S. Simula *et al.*, Phys. Rev. D **87** (2013) 114505 [arXiv:1303.4896 [hep-lat]].

[7] T. Ishikawa, T. Blum, M. Hayakawa, T. Izubuchi, C. Jung and R. Zhou, Phys. Rev. Lett. **109** (2012) 072002 [arXiv:1202.6018 [hep-lat]].

[8] S. Aoki, K. I. Ishikawa, N. Ishizuka, K. Kanaya, Y. Kuramashi, Y. Nakamura, Y. Namekawa and M. Okawa *et al.*, Phys. Rev. D **86** (2012) 034507 [arXiv:1205.2961 [hep-lat]].

[9] T. Blum, R. Zhou, T. Doi, M. Hayakawa, T. Izubuchi, S. Uno, N. Yamada, Phys. Rev. **D82** (2010) 094508. [arXiv:1006.1311 [hep-lat]].

[10] N. Tantalo, PoS LATTICE **2013** (2014) 007 [arXiv:1311.2797 [hep-lat]].

[11] A. Portelli, PoS LATTICE **2014** (2015) 013 [arXiv:1505.07057 [hep-lat]].

[12] F. Bloch and A. Nordsieck, Phys. Rev. **52** (1937) 54.

[13] J. Bijnens, Phys. Lett. B **306** (1993) 343 [hep-ph/9302217].

[14] J. Gasser and G. R. S. Zarnauskas, Phys. Lett. B **693** (2010) 122 [arXiv:1008.3479 [hep-ph]].

[15] F. Ambrosino *et al.* [KLOE Collaboration], Phys. Lett. B **632** (2006) 76 [hep-ex/0509045].

[16] F. Ambrosino *et al.* [KLOE Collaboration], Eur. Phys. J. C **64** (2009) 627 [Erratum-ibid. **65** (2010) 703] [arXiv:0907.3594 [hep-ex]].

[17] J. Bijnens, G. Ecker and J. Gasser, Nucl. Phys. B **396** (1993) 81 [hep-ph/9209261].

[18] J. Bijnens, G. Colangelo, G. Ecker and J. Gasser, 2nd DAPHNE Physics Handbook:315-389 [hep-ph/9411311].

[19] V. Cirigliano and I. Rosell, Phys. Rev. Lett. **99** (2007) 231801 [arXiv:0707.3439 [hep-ph]].

[20] S. M. Berman, Phys. Rev. **112** (1958) 267.

[21] T. Kinoshita and A. Sirlin, Phys. Rev. **113** (1959) 1652.

[22] J. Beringer *et al.* [Particle Data Group Collaboration], Phys. Rev. D **86**, 010001 (2012).

[23] A. Sirlin, Phys. Rev. D **22** (1980) 971.

[24] A. Sirlin, Nucl. Phys. B **196** (1982) 83.

[25] E. Braaten and C. -S. Li, Phys. Rev. D **42** (1990) 3888.

[26] M. Hayakawa and S. Uno, Prog. Theor. Phys. **120** (2008) 413 [arXiv:0804.2044 [hep-ph]].

[27] P. Boucaud *et al.* [ETM Collaboration], Phys. Lett. B **650** (2007) 304 [hep-lat/0701012].

[28] T. Kinoshita, Phys. Rev. Lett. **2** (1959) 477.